

# Broadband Miniaturized Efficient Array Antennas

Amir Jafargholi<sup>1</sup> and Ali Jafargholi<sup>2</sup>

<sup>1</sup>Institute of Space Science and Technology  
Amirkabir University of Technology, 424 Hafez Ave., P. O. Box: 15875-4413, Tehran, Iran  
jafargholi@ieee.org

<sup>2</sup>Department of Electrical Engineering  
Sharif University of Technology, Azadi Ave., P. O. Box: 11365-11155. Tehran, Iran  
jafargholi@sharif.edu

**Abstract** — This paper introduces a new array architecture, in which antenna elements are arranged in a spiral curve. The spiral array enhances ultra-wideband (UWB) pattern characteristics compared to alternative array geometries of similar elements, without requiring a complex feed network for frequency change compensation. A number of examples are illustrated to demonstrate the array capability in broadband array designs. It is revealed that for the same number of elements and curvature lengths, a spiral array has a wider radiation bandwidth than the corresponding circular and linear array antennas. In addition, it is also demonstrated that the spiral architecture discussed here can be best suited for small antenna array applications. Simulations show that different spiral parameters lead to different size reduction, which vary from 30% to 90% with regards to a conventional circular array antenna.

**Index Terms** - Miniaturized array antenna, spiral array antenna, and ultra-wide band.

## I. INTRODUCTION

Array elements, feed networks, and array architecture are three main factors determining the array size and its performance [1]. There is renewed interest in non-foster circuitry for antennas lately [2-6]. The antenna size implies limitations in bandwidth and gain characteristics. However, if non-foster/negative circuits are employed such restrictions can be partially overcome. As an important parameter in the array

design, the feed network generally depends on the array elements and architecture. The selection of the array architecture for the realization of a desired array antenna is determined by requirements on the array bandwidth, pattern, size, and scan range [1]. In addition, broad radiation and input impedance bandwidths are two major characteristics of the antenna arrays for broadband applications. Since the input impedance bandwidth depends on the characteristics of the element used in the array, the radiation bandwidth is the limiting factor. In other words, the radiation bandwidth of the array limits its practical bandwidth. Since antenna arrays play a significant role, both in direction finding and in increasing the capacity of the systems, the use of suitable array architecture is becoming increasingly important. From an architecture point of view, there are still many theoretical as well as practical open issues despite the basic configurations found in the literature [1].

The broadband frequency characteristics can be obtained based on the fundamental theory introduced by Rumsey in the fall of 1954 [7]. As a result, we speculate that the spiral array architecture, in which antenna elements are arranged in a spiral curve, may be frequency independent. The simulation results confirmed this claim [8-9]. The proposed spiral architecture exhibits a great potential for applications such as radio direction finding and UWB systems. In UWB systems, one is interested in having an antenna or antenna array, which maintains a substantially stable radiation pattern over the entire frequency range of interest to keep UWB pulse distortion as small as possible.

However, the bandwidth of conventional arrays (linear and circular arrays) is limited because the radiation pattern scans with frequency and thus moves off the target. In order to avoid this beam squint problem, wide band arrays are required.

In this paper, the miniaturization capability of the proposed spiral architecture as compared to conventional linear and circular arrays has been considered. Simulation shows that the spiral architecture can be best suited for small antenna array applications. They show that different spiral parameters lead to different size reduction, which vary from 30% to 90% with regards to a conventional circular array antenna.

## II. ARRAY ANTENNA FORMULATION

Considering an  $m$ -element simple spiral-array antenna, the position vector may be written as,

$$\vec{r}_m = \vec{r} e^{a\phi_m} = r_0 e^{a\phi_m} \cos(\phi_m) \hat{x} + r_0 e^{a\phi_m} \sin(\phi_m) \hat{y} \quad (1)$$

here,  $a$  is the spiral constant and specifies the increasing rate of the spiral radius proportionate with angle  $\phi_m$ ,  $x_m$ , and  $y_m$  are the cartesian location of the array elements, and  $\vec{r}$  is the vector of the spiral constellation. In Fig. 1,  $r_0$  is the distance of the first element of the array from the origin, and  $\phi_m = \frac{(m-1)\pi}{b}$  represents the angle of the  $m^{th}$  element

in polar coordinate, where parameter  $b$  may be chosen arbitrarily in order to make a smoother change in spiral contour and to increase the degrees of freedom in the design.

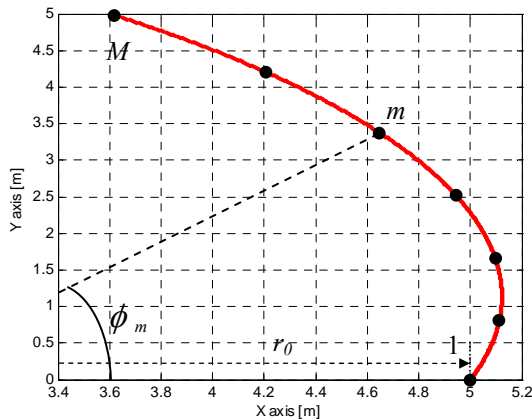


Fig. 1. Two possible array architectures, where the element locations are specified by equation (2):  $a = 0.221$ ,  $M = 7$ ,  $b = 20$ ,  $f_0 = 30$  MHz, and  $r_0 = 5$  m.

It should be noted that  $b$  has a positive value. The array factor of the spiral array is [8],

$$AF(\theta, \phi) = \sum_{m=1}^M I_m e^{j\left(\frac{2\pi}{\lambda} r_0 e^{a\phi_m} \sin \theta \cos(\phi - \phi_m) + \delta_m\right)} \quad (2)$$

The spiral array bandwidth has been calculated in before, [8-Appendix]. In order to gain further insight into the spiral array bandwidth, equation (3) introduces a spiral to linear bandwidth ratio (SLBWR)

$$SLBWR = \frac{\frac{1}{2} M (M + 1) \left( e^{\frac{a\pi}{b}} - 1 \right)}{\left[ e^{\frac{a\pi}{b} M} - 1 \right]} \quad \text{For } r_0 = d_{Linear} \quad (3)$$

where,  $d_{Linear}$  is the element separation for the linear array.

## III. ARRAY SYNTHESIS AND SIMULATION RESULTS

To verify the array performance, a 7 element spiral array antenna, with parameters  $r_0 = \lambda_c/2$ ,  $a = 0.221$ , and  $b = 20$ , where the desired frequency  $f_c = 30$  MHz and  $\lambda_c = 10$  m, has been first analytically studied (Fig. 1). A comparison has been done using the simulation results obtained by SuperNEC software. Using equation (1), the element locations are specified in Table 1. According to the progressive-phase excitation method and uniform amplitude, for the main lobe located at  $(\theta_0, \phi_0)$  the phase  $\delta_m$  for each element can be expressed as [7],

$$\delta_m = -\frac{2\pi}{\lambda} r_0 e^{a\phi_m} \sin \theta_0 \cos(\phi_0 - \phi_m) \quad (4)$$

For the main lobe, which is directed to  $(\theta_0, \phi_0) = (90^\circ, 90^\circ)$ , the array feed values are specified in Table 1. The analytic results for  $f = 10, 20, 30, 40$ , and 50 MHz are shown in Fig. 2. To simulate the structure with the aid of SuperNEC, the array elements are located on infinite perfect ground, and the length of monopole antennas is chosen to be  $L = 2$  m. We have chosen monopole antennas (with omni-directional radiation patterns over the entire frequency band) as array elements instead of conventional broadband elements. In addition, we assumed in simulations that the impedance of elements is matched over the entire frequency band. Small changes in radiation patterns over the entire frequency band, 10–50 MHz, make the proposed array applicable as an ultra-wideband

array antenna. In Fig. 3, a comparison between the analytic and numeric (SuperNEC simulation results) simulations is presented. As can be seen clearly, the simulated results obtained by SuperNEC software show good agreement with the analytic calculations.

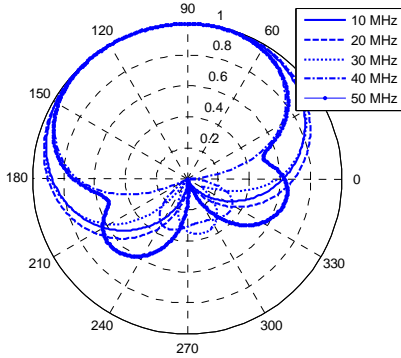


Fig. 2. A seven element spiral array architecture;  $a = 0.221$ ,  $M = 7$ ,  $b = 20$ , and  $\theta = 90^\circ$  plane.

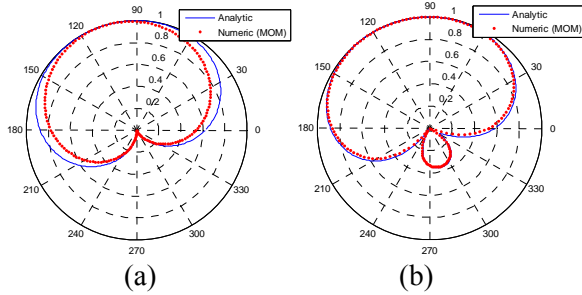


Fig. 3. Analytic and numeric (SuperNEC) simulation results comparison,  $L = 2\text{m}$ , for (a) 10MHz and (b) 30 MHz.

Table 1: Spiral array elements properties for 10 – 50 MHz.

Element No.	Location, (x) (m)	Location, (y) (m)	Current
1	5.0	0	1.0
2	5.11	0.81	0.873-0.487i
3	5.09	1.65	0.506-0.863i
4	4.94	2.52	-0.012-1.0i
5	4.65	3.37	-0.523-0.852i
6	4.20	4.21	-0.878-0.478i
7	3.62	4.98	-1.0-0.01i

## IV. COMPARISON OF SPIRAL, CIRCULAR, AND LINEAR ARRAY ARCHITECTURES

Various array architectures have been proposed and investigated in the literature [1, 8]. Besides the spiral array architecture proposed in this paper, the linear and circular array architectures are popularly used in antenna engineering.

In this section, two different high (1–10 GHz) and low (10–50 MHz) frequency architecture have been studied. Moreover, to compare them with linear and circular array antennas two different scenarios have been choose: equivalent and different array lengths conditions.

### A. Equivalent array length

In [7–Fig. 8], the geometries of the spiral, linear, and circular arrays have been compared. To make a fair comparison, the number of elements and curvature lengths are the same in all cases. The total length of an  $M$  element linear array with an element separation of  $d_{Linear}$  is  $L = (M-1)d_{Linear}$  while the circumference of an  $M$  element circular array with a radius of  $r_0$  is  $C_S = 2\pi r_{0,Circular}$ . In addition, for an  $M$  element spiral array, the array circumference can be expressed by equation (5),

$$C_S = \frac{r_0 \sqrt{1+a^2}}{a} (e^{a\phi_M} - 1). \quad (5)$$

To have a fair comparison, the element separation for linear array and the radius of the circular array are selected to satisfy equation (6)

$$\begin{aligned} r_{0,Circular} &= C_S \cdot \frac{1}{2\pi}, \\ d_{Linear} &= C_S \cdot \frac{1}{(M-1)}. \end{aligned} \quad (6)$$

The parameters of the spiral array are:  $M = 5$ ,  $r_0 = 0.04$  m,  $a = -0.125$ , and  $b = 1.75$ , where the desired frequency is  $f_c = 5$  GHz. The configuration of the spiral, circular and linear arrays are labeled in [7–Fig. 8]. For all array geometries, simple monopole antennas are used as array elements. The directivity of these arrays for the main beam direction is plotted in [7–Fig. 9 (a)]. As revealed in the figure, the spiral array architecture provides a wider radiation bandwidth.

The 3 dB radiation bandwidth of the spiral array architecture is approximately 4.1 and 1.9 times wider than that of the linear and circular

arrays, respectively. Finally, it should be noted that the spiral arrangement allows the beam to be steered in any direction in the azimuth plane, similar to the linear and circular arrangements [1].

**B. Different array lengths**

Now, we compare the gain of a seven element spiral array antenna,  $r_0 = \lambda_c/2$ ,  $a = 0.221$ , and  $b = 20$ , for the frequency  $f_c = 30$  MHz and  $\lambda_c = 10$  m, with that of linear and circular array (see Fig. 4). The distance between the elements of the linear array is  $r_0 = \lambda_c/2 = 5$  m, whereas elements of the circular array are located on a circle with a radius of  $r = \lambda_c$ , with all of the elements having a 2 m length. As it seems in Fig. 5, the gain of the spiral array antenna changes smoothly over the entire frequency range, and consequently its 3 dB bandwidth is considerably greater than that of linear and circular arrays. It should be also considered that the gain of linear and circular arrays is not constant and fluctuate rapidly over the frequency range. The present result shows that the array bandwidth is defined over 10 MHz-35 MHz range and confirms SLBWR (equation (3), which is approximately 3.5:1). The arrays have been designed for the main lobe location in  $(\theta_0, \phi_0) = (90^\circ, 90^\circ)$  and the feeding values for these elements are also specified in Table 1.

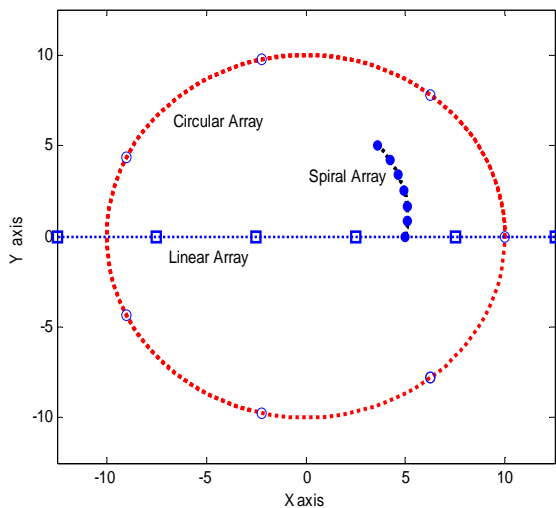


Fig. 4. The geometries of the spiral, circular, and linear arrays.

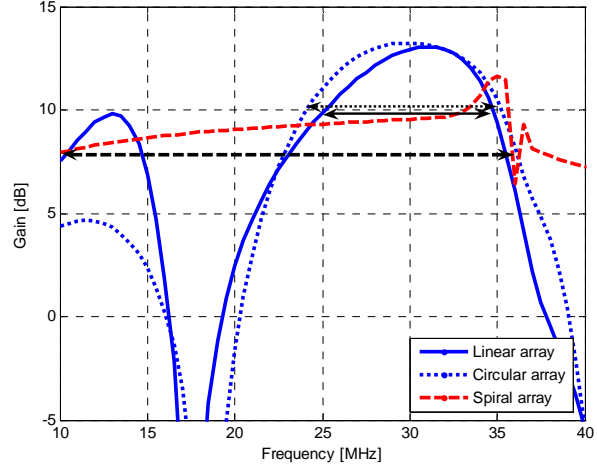


Fig. 5. Comparison between the directivity of different array geometries in the main lobe ( $\theta = 90^\circ, \phi = 0^\circ$ ) direction.

**V. MINIATURIZATION CHARACTERISTIC**

A comparison between circular and spiral array antennas has been presented before. It is shown that for the array with same number of elements and uniform feeding, the suggested spiral array is much more miniaturized than the simple linear and circular array architectures. Due to this fact that the linear array has worst condition in array miniaturization capability, here, we just studied the circular and spiral array antenna.

To have a better insight, again we investigated an equivalent, smaller and much smaller spiral array length with regards to a conventional circular array antenna. In each case, the radiation pattern, the array size, and its frequency bandwidth have been considered.

In Figs. 6, 7, and 8, we assumed that the desired main lobe is located in (a)  $(\theta_0, \phi_0) = (90^\circ, 90^\circ)$ , (b)  $(\theta_0, \phi_0) = (45^\circ, 45^\circ)$ , and (c)  $(\theta_0, \phi_0) = (60^\circ, 30^\circ)$ . The elements of the circular array are located on a circle with radius of  $r = \lambda_c$ , where the desired frequency is  $f_c = 300$  MHz ( $\lambda_c = 1$  m). In these figures, a simple spiral array antenna that has (a) 7 elements, with  $r_0 = \lambda_c/4$ ,  $a = -0.0221$ , and  $b = 3$ ; (b) 15 elements, with  $r_0 = \lambda_c$ ,  $a = -0.1221$ , and  $b = 4$ ; and (c) 15 elements, with  $r_0 = \lambda_c/3$ ,  $a = -0.221$ , and  $b = 7$ , has been compared with the same element number circular array antennas.

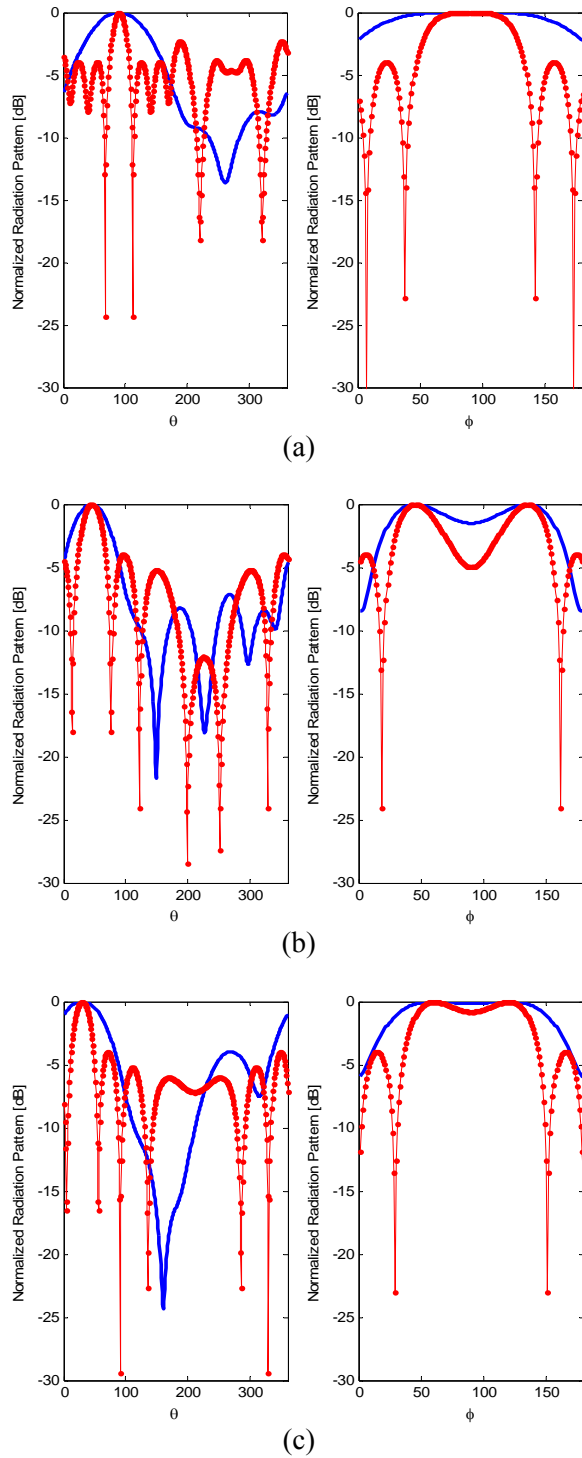


Fig. 6. Normalized radiation pattern comparison with uniform feeding in both the E- and H-planes, (solid) spiral and (dotted solid) circular array antennas for (a)  $(\theta_0, \phi_0) = (90^\circ, 90^\circ)$ , (b)  $(\theta_0, \phi_0) = (45^\circ, 45^\circ)$ , and (c)  $(\theta_0, \phi_0) = (60^\circ, 30^\circ)$ .

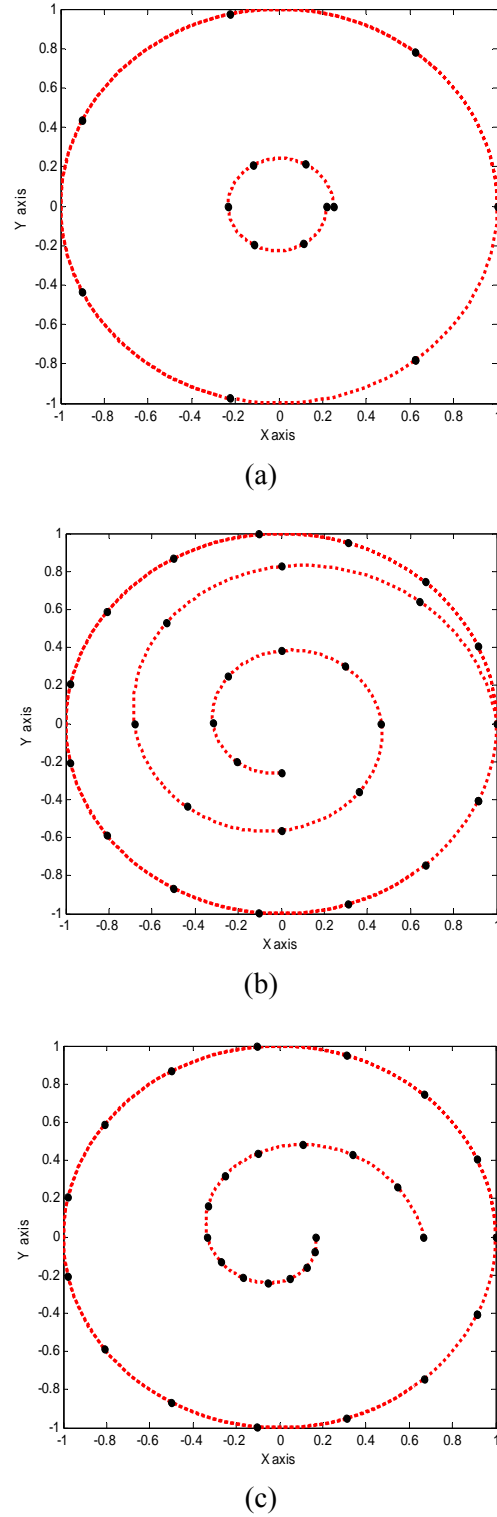


Fig. 7. (a) 7 and 15 elements spiral and circular array, (b) type I, and (c) type II.

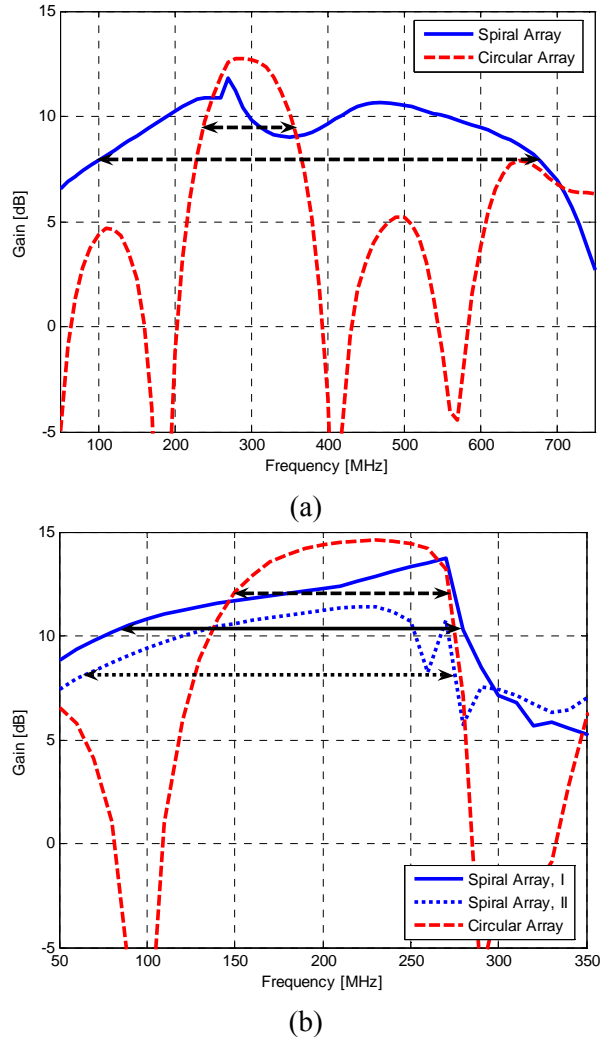


Fig. 8. Gain comparison for the desired main beam direction,  $f_{high}/f_{low}$  = (a) 1.49 for circular and 6.75 for spiral, (b) 1 for circular, 3.1 for type I and 4.46 for type II.

In these figures, the array radiation, architecture and size have been compared. It seems clearly that the spiral array antenna has been miniaturized with regards to simple circular array; whereas it approximately achieves the same radiation characteristics and even though broader bandwidth as shown in Fig. 6. From Fig. 7, over 90 %, 30 %, and 70 % size reductions have been achieved for the respective designed spiral array architectures. In Fig. 8, the gain of the arrays in the desired main beam direction has been compared. It seems that the array bandwidth ( $f_{high}/f_{low}$ ) for circular and spiral cases are: (a) 1.49 and 6.75, (b) 1 for circular, 3.1 for type I and 4.46 for type II, respectively.

## VI. CONCLUSION

In this paper, a novel planar array for broadband applications has been introduced and thoroughly investigated. A fair comparison between the spiral array architecture and its conventional counterparts, exhibits the ability of the proposed architecture to enhance the radiation bandwidth of an array. Several spiral array antennas have been designed and simulated to confirm the theoretical calculations. We also investigated the array miniaturization capability. Simulations show that choosing optimum parameters leads to array size reduction, which is vary from 30 % to 90 %.

## REFERENCES

- [1] B. Allen, M. Dohler, E. E. Okon, W. Q. Malik, A. K. Brown, and D. J. Edwards, *Ultra-Wideband Antennas and Propagation for Communications, Radar and Imaging*, John Wiley, 2007.
- [2] J. T. Aberle, "Two-port representation of an antenna with application to non-foster matching networks," *IEEE Trans. Antennas Propag.*, vol. 56, no. 5, pp. 1218-1222, 2008.
- [3] R. Ziolkowski, P. Jin, and C. Lin, "Metamaterial-inspired engineering of antennas," *Proc. IEEE*, vol. 99, pp. 1720-1731, 2011.
- [4] P. Jin and R. Ziolkowski, "Broadband, efficient, electrically small metamaterial-inspired antennas facilitated by active near-field resonant parasitic elements," *IEEE Trans. Antennas Propag.*, vol. 58, pp. 318-327, 2010.
- [5] N. Zhu and R. W. Ziolkowski, "Active metamaterial-inspired broad bandwidth, efficient, electrically small antennas," *IEEE Antennas Wireless Propag. Lett.*, vol. 10, pp. 1582-1585, 2011.
- [6] S. E. Sussman-Fort and R. M. Rudish, "Non-foster impedance matching of electrically-small antennas," *IEEE Trans. Antennas Propag.*, vol. 57, no. 8, pp. 2230-2241, 2009.
- [7] J. D. Dyson, "The equiangular spiral antenna," *IEEE Trans. Antennas Propag.*, vol. 7, no. 2, pp. 181-187, 1959.
- [8] A. Jafargholi, M. Kamyab, and M. Veysi, "Spiral array architecture, design, synthesis and application," *IET Microwave Antenna Propag.*, vol. 5, pp. 503-511, April 2011.
- [9] A. Jafargholi and M. Kamyab, "Pattern optimization in an UWB spiral array antenna," *Progress In Electromagnetics Research M*, vol. 11, pp. 137-151, 2010.



**Amir Jafargholi** received the Ph.D. degree in Electrical Engineering from K. N. Toosi University of Technology, Tehran, Iran, in 2011. He is the coauthor of about 50 scientific contributions published in international books, journals and peer-reviewed conference proceedings. His research interest includes the applications of metamaterials in the analysis and synthesis of antennas.

Dr. Jafargholi was a recipient of a Student's Best Thesis National Festival award for his B.Sc thesis, on May 2006. He was a recipient of the 22<sup>th</sup> Khawarizmi International and 13<sup>th</sup> Khawarizmi Youth Award on Jan. 2009 and Oct. 2011, respectively. He was also the recipient of Research Grant Awarded in Metamaterial 2010.



**Ali Jafargholi** was born in Tehran, Iran, on November 3, 1989. He received the B.Sc. degree in Electrical Engineering from Sharif University of Technology, Tehran, Iran, in 2012, and is currently working toward the M.Sc. degree in Communication Engineering. His research interests include metamaterial applications to antenna designs.